



# Synthesis, characterization and application of nano-sized $\text{Co}_2\text{CrO}_4$ spinel catalyst for selective oxidation of sulfides to sulfoxides

Mohammad Yazdanbakhsh<sup>\*</sup>, Iman Khosravi, Mahboobeh-Sadat Mashhoori,  
Mohammad Rahimizadeh<sup>\*</sup>, Ali Shiri, Mehdi Bakavoli

Department of Chemistry, Faculty of Sciences, Ferdowsi University of Mashhad, 91775-1436 Mashhad, Iran

## ARTICLE INFO

### Article history:

Received 16 April 2011

Received in revised form 27 August 2011

Accepted 28 October 2011

Available online 7 November 2011

### Keywords:

- A. Nanostructures
- A. Oxides
- B. Chemical synthesis
- B. Sol–gel chemistry
- D. Catalytic properties

## ABSTRACT

The nano-sized  $\text{Co}_2\text{CrO}_4$  spinel was produced for the first time by thermal decomposition of Cr–Co gel prepared by sol–gel method. It was shown that well-crystallized spinel structure is formed after calcination at 450 °C. The usual characterizations were performed and the results showed the particle size of the prepared spinel is 9 nm. Moreover, the prepared nano-sized  $\text{Co}_2\text{CrO}_4$  spinel was applied in a simple, efficient and recyclable method for selective oxidation of sulfides to their corresponding sulfoxides with aqueous hydrogen peroxide in *tert*-butanol.

© 2011 Elsevier Ltd. All rights reserved.

## 1. Introduction

Spinel compounds have a general formula of  $\text{AB}_2\text{O}_4$  in which A is a divalent metal and B is a trivalent one. Spinels containing transition metal ions like  $\text{Co}^{\text{II}}\text{Co}^{\text{III}}\text{Cr}^{\text{III}}\text{O}_4$  can act as efficient catalysts in a number of heterogeneous chemical processes such as CO oxidation [1], catalytic combustion of hydrocarbons [2] and reduction of several organic compounds [3]. A variety of methods have been applied to prepare spinel compounds such as the ceramic route which is the most general method for preparing spinels involves the solid-state reaction of mechanically mixed parent metal oxides. In this method, a temperature of about 1027 °C has to be maintained in order to complete the reaction [4,5]. On the other hand, the disadvantages of solid-state route such as inhomogeneity, lack of stoichiometry control and larger particle size are avoided when the material is synthesized with solution-based method [6]. Moreover,  $\text{Co}_2\text{CrO}_4$  spinel has been prepared by the methods including high-temperature calcination of hydroxide or carbonate precursor mixtures [7], typical coprecipitation [8] and hydrothermal synthesis [9]. The particle size of  $\text{Co}_2\text{CrO}_4$  spinel obtained by these methods is usually in the range of 0.1–1  $\mu\text{m}$ . An alternative method for Cr–Co spinel formation would be the sol–gel method using oxalic acid as a

chelating agent and low-temperature calcination. However, the preparation of spinel-type  $\text{Co}_2\text{CrO}_4$  nanoparticles using the latter method has not been reported elsewhere.

## 2. Experimental

The decomposition and reaction processes of the dried polymeric gel were analyzed by differential thermal analysis (DTA) method in air and in the thermal range of 20–1000 °C at a heating rate of 10 °C  $\text{min}^{-1}$  using a NETZSCH instrument. To study the phase transformation, crystallization and sinter ability of the derived powders, the complex polymeric gel was decomposed at various temperatures for 2 h. The complex polymeric gel and derived powders were also analyzed by Fourier transform infrared (FTIR) spectroscopy on thermo Nicolet Nexus 870 FTIR spectrometer. The crystallization and microstructure of the oxide nanopowders were characterized with an X-ray diffractometer employing a scanning rate of 0.02  $\text{s}^{-1}$  using an X'pert, Philips, equipped with  $\text{CuK}_\alpha$  radiation. The data were analyzed using JCPDS standards. The morphology and dimension of the nanoparticles were observed by transmission electron microscope (TEM) which was taken on a LEO 912 AB TEM using an accelerating voltage of 120 kV. Samples for TEM were prepared by sonicating small amounts of the nanopowder in 5 ml of ethanol for 30 min and then a few drops of the suspension were deposited on a holey carbon grid. The visible and UV absorption spectra were measured using Agilent 8453 UV/vis/NIR spectrophotometer in the range of 200–800 nm. The specific surface area (SSA)

<sup>\*</sup> Corresponding authors. Tel.: +98 5118797022; fax: +98 5118796416.  
E-mail addresses: [myazdan@ferdowsi.um.ac.ir](mailto:myazdan@ferdowsi.um.ac.ir), [myazdan@um.ac.ir](mailto:myazdan@um.ac.ir)  
(M. Yazdanbakhsh), [rahimizh@yahoo.com](mailto:rahimizh@yahoo.com) (M. Rahimizadeh).

of the catalyst was calculated using BET method from the nitrogen adsorption isotherms obtained at 77 K on samples outgassed at 150 °C by Autosorb 1-C.

### 2.1. Preparation of $\text{Co}_2\text{CrO}_4$ nanopowders

To a magnetically stirred solution of  $\text{Cr}(\text{NO}_3)_2 \cdot 6\text{H}_2\text{O}$  (0.005 mol, 2.0 g) and  $\text{Co}(\text{NO}_3)_2 \cdot 6\text{H}_2\text{O}$  (0.01 mol, 2.9 g) in ethanol (20 ml), a solution of oxalic acid (0.15 mol, 1.9 g) in ethanol (10 ml) was slowly added. The mixture was stirred at room temperature for 5 h before the solvent was evaporated at 80 °C. After forming the sol, it was heated at 120 °C until the gel formed. It was subsequently dried and ground in order to attain the oxalate precursor powder. The resulting material was eventually calcined at 450 °C for 8 h and the well-crystallized spinel was obtained.

### 2.2. General procedure for the oxidation of sulfides to sulfoxides 2(a–l)

To a stirred mixture of sulfide **1(a–l)** (1 mmol) and nano-sized  $\text{Co}_2\text{CrO}_4$  spinel (0.5 mol%, 1.1 mg) in *t*-BuOH (10 ml), a solution of 30%  $\text{H}_2\text{O}_2$  (10 equiv.) was added gradually at room temperature. After the completion of the reaction which was monitored by TLC using *n*-hexane:ethyl acetate (2:1), the catalyst was centrifuged off. The organic phase was evaporated and then  $\text{CH}_2\text{Cl}_2$  (20 ml) was added to the resultant. The solution was washed with water ( $2 \times 10$  ml) and dried over anhydrous  $\text{Na}_2\text{SO}_4$ . The solvent was removed under reduced pressure to afford the crude product. Further purification was performed by column chromatography using *n*-hexane:ethyl acetate (5:1) as an eluent. The spectral data of the purified compounds were in accordance with those of the authentic samples.

## 3. Results and discussion

### 3.1. Thermal analysis

Fig. 1 shows the DTA curve of the  $\text{Co}_2\text{CrO}_4$  gel precursor obtained by the sol–gel method. It shows a large endothermic peak around 150 °C which is assigned to the evaporation of ethanol. The exothermic peak around 270 °C might be owing to the combustion of the organic compounds such as oxalic acid and the residual ethanol. The small exothermic peak at 370 °C can be attributed to the decomposition of nitrate ion which is decomposed completely around 420 °C and resulted in a broad exothermic peak [10]. No obvious change was observed above 470 °C. Hence, the lowest calcination temperature is about 450 °C.

### 3.2. X-ray diffraction studies

Fig. 2 shows the X-ray diffraction patterns of the  $\text{Co}_2\text{CrO}_4$  spinel formed when the gel was calcined at 450 °C for 8 h. The diffraction peaks at  $2\theta$  angle which appeared at 18.91, 31.05, 36.54, 38.19, 44.31, 55.00, 58.75 and 64.32° can be assigned to scatter from the (1 1 1), (2 2 0), (3 1 1), (2 2 2), (4 0 0), (4 2 2), (5 1 1) and (4 4 0) planes of the spinel crystal lattice, respectively.

The peaks of the XRD spectrum confirm clearly that the phases belonging to  $\text{Co}_2\text{CrO}_4$  match well with the phases reported in the powder diffraction database. The data of XRD show that  $\text{Co}_2\text{CrO}_4$  crystallizes in a cubic phase with  $a = 8.1700$  Å. A lattice structure in which the tetrahedral positions of a normal spinel are occupied by  $\text{Co}^{2+}$  and the octahedral positions by  $\text{Cr}^{3+}$  and  $\text{Co}^{3+}$  is proposed as the only structure consistent with both the observed X-ray data and previously established structures of multiple metal oxides of  $\text{Co}^{2+}$  and  $\text{Co}^{3+}$  [11,12].

The crystallite sizes were calculated from the (3 1 1) peak of XRD using Scherer's equation (Eq. (1)): where  $D_{hkl}$  is the particle

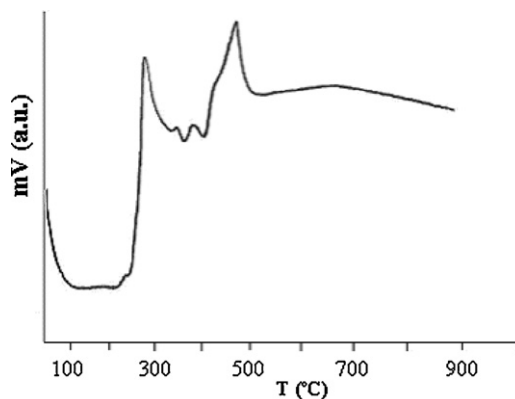


Fig. 1. DTA curve of the  $\text{Co}_2\text{CrO}_4$  precursors obtained by the sol–gel method.

size perpendicular to the normal line of (*h k l*) plane,  $\beta_{hkl}$  is the full width at half maximum,  $\theta_{hkl}$  is the Bragg angle of (*h k l*) peak, and  $\lambda$  is the wavelength of X-ray.

$$D_{hkl} = \frac{0.9\lambda}{\beta_{hkl} \cos \theta_{hkl}} \quad (1)$$

The particle sizes of  $\text{Co}_2\text{CrO}_4$  nanoparticles calcined at 450 °C are 9 nm. The specific surface area (SSA) measured by BET measurements was about 51.75  $\text{m}^2 \text{g}^{-1}$ .

### 3.3. IR spectra of dried gel and annealed particles

The nanopowder of  $\text{Co}_2\text{CrO}_4$  spinel was also characterized by IR spectroscopy. The spectrum of the nanopowder in Fig. 3 shows that there are two strong absorption bands at 656 and 561  $\text{cm}^{-1}$  which coincide with those reported for  $\text{Co}_2\text{CrO}_4$  spinel in the literature [13]. The peak at 656  $\text{cm}^{-1}$  is attributed to the stretching vibration mode of M–O for the tetrahedrally coordinated metal ions and the

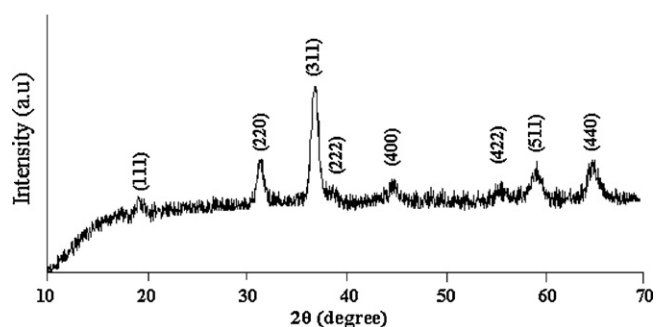


Fig. 2. XRD patterns of the  $\text{Co}_2\text{CrO}_4$  nanopowders sintered at 450 °C.

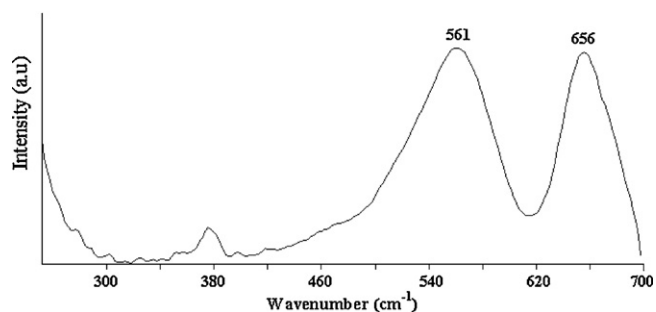


Fig. 3. Far-IR spectrum of nano-sized  $\text{Co}_2\text{CrO}_4$  spinel.

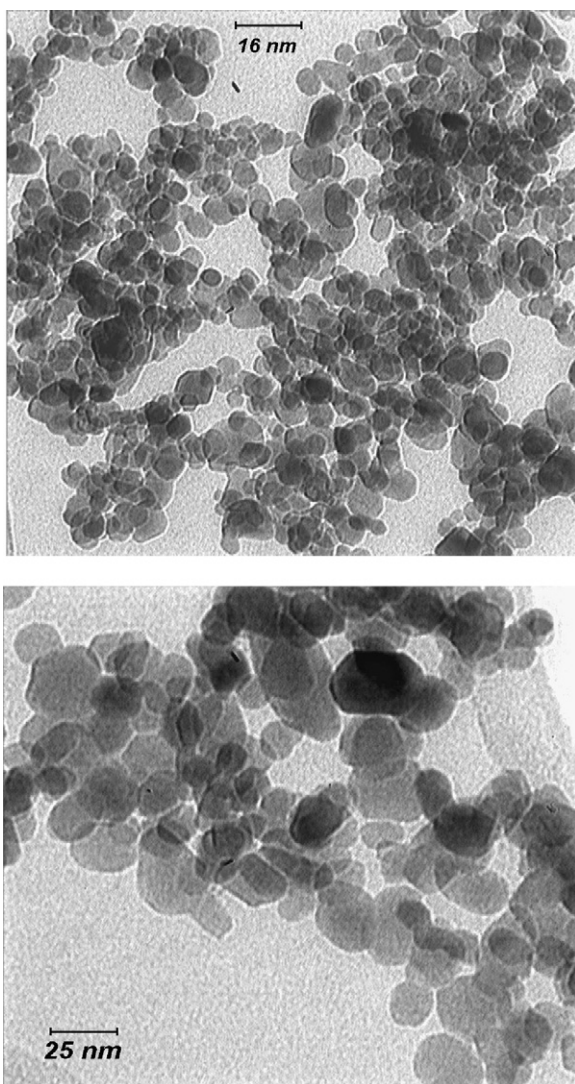


Fig. 4. TEM images of nano-sized  $\text{Co}_2\text{CrO}_4$  spinel calcined at  $450^\circ\text{C}$  in two magnifications.

band at  $561\text{ cm}^{-1}$  can be assigned to the octahedrally coordinated metal ions.

### 3.4. Powder morphology

Fig. 4 shows the TEM images of  $\text{Co}_2\text{CrO}_4$  spinel nanoparticles with two different magnifications. According to TEM images, the morphology of nanoparticles is homogeneous and the spinel nanoparticles consist of uniform quasi-spherical crystallites with an average size of 9 nm. This value is in agreement with the XRD results.

In addition, energy-dispersive X-ray (EDX), as shown in Fig. 5, confirmed the expected Co to Cr ratio as well as the phase-purity of the nanopowders. In order to confirm the homogeneous distribution of the constituting elements, EDX analysis was performed on various particles having well defined morphology within different clusters which these results in conjunction with XRD results confirmed the chemical homogeneity of the synthesized nano-sized  $\text{Co}_2\text{CrO}_4$  spinel by this procedure.

### 3.5. Optical properties

An estimate of the optical band gap,  $E_g$ , can be determined via UV–vis spectroscopy by the following equation for direct

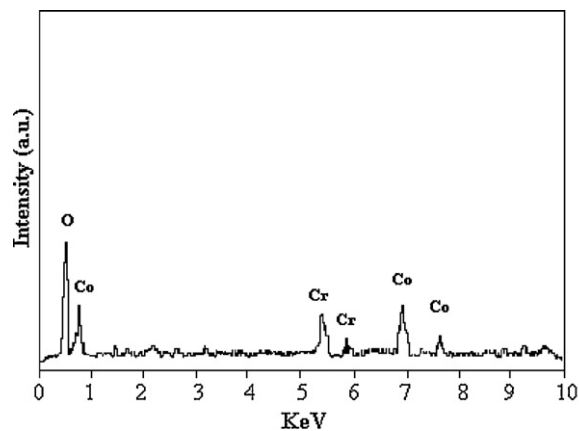


Fig. 5. EDX pattern of nano-sized  $\text{Co}_2\text{CrO}_4$  spinel.

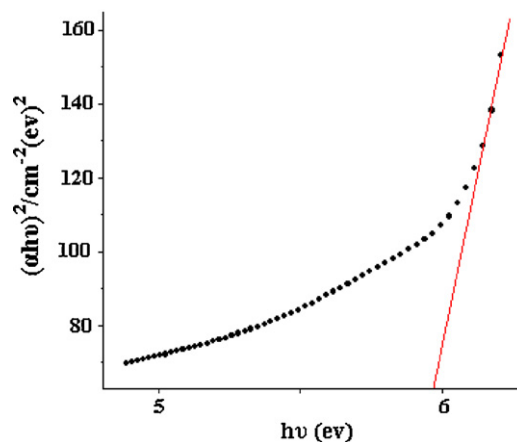


Fig. 6. Dependence of  $(\alpha h\nu)^2$  on the photon energy ( $h\nu$ ) for nano-sized  $\text{Co}_2\text{CrO}_4$  spinel.

semiconductor:

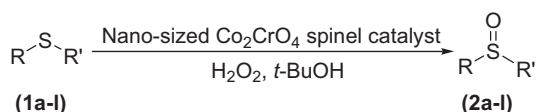
$$(\alpha h\nu)^2 = C(h\nu - E_g) \quad (2)$$

where  $h\nu$  is the photon energy,  $\alpha$  is the absorption coefficient and  $C$  is a constant. The value of the optical band gap can be calculated by plotting  $(\alpha h\nu)^2$  versus photon energy (Fig. 6). This value is 5.82 eV.

### 3.6. Catalytic application of $\text{Co}_2\text{CrO}_4$ spinel nanoparticles in selective oxidation of sulfides to sulfoxides 2(a–l)

The attempt for discovery of new nano metal oxides for catalytic applications in organic chemistry is one of the current challenges in heterogeneous catalysis. This is because of their advantages like easy workup, reusability, atom economy and reduction of waste. These compounds have also extraordinary properties relative to their corresponding bulk materials. Due to their unusual physical and chemical catalytic properties [14–16], they act as promising catalysts because of their high activity, non-toxicity, ease of availability, strong oxidizing power and long-term stability [17–19]. In view of these facts and in the continuation of our previous work [20–22], we investigated the role of  $\text{Co}_2\text{CrO}_4$  spinel nanopowder in selective oxidation of sulfides to their corresponding sulfoxides with aqueous  $\text{H}_2\text{O}_2$  as an eco-friendly green oxidant (Scheme 1).

The oxidation of methyl phenylsulfide with 30% hydrogen peroxide using  $\text{Co}_2\text{CrO}_4$  spinel nanoparticles as a catalyst was examined in several solvents (Table 1). The less polar solvents



Scheme 1.

Table 1

Solvent optimization on chemoselective oxidation of methyl phenylsulfide to methyl phenylsulfoxide.<sup>a</sup>

Entry	Solvent	Sulfide (%) <sup>b</sup>	Sulfoxide (%)	Sulfone (%)
1	Hexane	72	23	5
2	CH <sub>2</sub> Cl <sub>2</sub>	45	52	3
3	CHCl <sub>3</sub>	40	55	5
4	THF	15	83	4
5	CH <sub>3</sub> CN	0	80	20
6	<i>t</i> -Butanol	1	99	0
7	MeOH	0	43	57
8	Acetone	0	26	74
9	AcOH	0	70	30

<sup>a</sup> All the reactions were carried out with 1 mmol of methyl phenylsulfide, 5 mg of nano-sized Co<sub>2</sub>CrO<sub>4</sub> spinel in 10 ml of solvent and 10 equiv. of 30% aqueous hydrogen peroxide at room temperature after 1 h.

<sup>b</sup> Selectivities are based on <sup>1</sup>H NMR spectroscopic integration.

constituting a heterogeneous solvent system with aqueous hydrogen peroxide were not effective (entries 1–4). In the polar solvents, methyl phenylsulfide was mostly overoxidized into its corresponding sulfone (entries 7–9). The oxidative ability of this reaction system in more polar solvents is greater than that in less polar solvents. Therefore, the best condition to prepare methyl phenylsulfoxide selectively is the reaction in *t*-BuOH at room temperature (entry 6). We think the lipophilicity and hydrophilicity of *t*-BuOH are appropriate for dissolving liquid phase and substrate as well as making an appropriate interaction with the surface of the nano catalyst.

The amount of the catalyst in the oxidation of thioanisole was also optimized. The results showed that when 0.5 mol% of nano catalyst was used in the oxidation of thioanisole with 10 equiv. of H<sub>2</sub>O<sub>2</sub>, the highest yield is obtained. When the reaction was carried out in the absence of catalyst at room temperature, the oxidation was not completed (Table 2). Also, the mentioned oxidation reaction was monitored in the presence of nano catalyst without H<sub>2</sub>O<sub>2</sub> as the control reaction. The results showed the oxidation reaction is not preceded even after two days.

To study the generality of the method, the synthesized Co<sub>2</sub>CrO<sub>4</sub> spinel nanoparticle with a variety of sulfides containing

Table 2

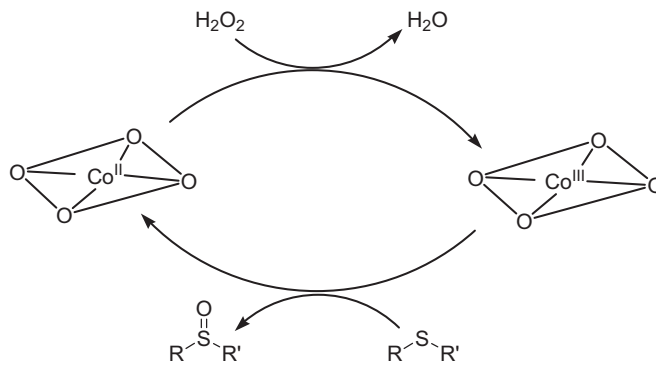
The data for the oxidation of methyl phenylsulfide.<sup>a</sup>

Entry	Molar ratio of catalyst (%)	H <sub>2</sub> O <sub>2</sub> (equiv.)	Sulfide (%) <sup>b</sup>	Sulfoxide (%)	Sulfone (%)
1	0	10	31	52	17
2	0.25	10	23	64	13
3	0.5	10	1	99	0
4	0.75	10	1	96	3
5	1	10	1	97	2
6 <sup>c</sup>	0.5	0	98	2	0
7	0.5	5	22	73	5
8	0.5	15	0	86	14
9	0.5	20	0	89	11

<sup>a</sup> All the reactions were carried out with 1 mmol of methyl phenylsulfide in *t*-BuOH at room temperature with 30% aqueous hydrogen peroxide after 1 h.

<sup>b</sup> Selectivities are based on <sup>1</sup>H NMR spectroscopic integration.

<sup>c</sup> The reaction was not preceded even after 2 days.



Scheme 2.

aromatic and aliphatic moieties were subjected to oxidation reaction using H<sub>2</sub>O<sub>2</sub> as the oxidant. Table 3 shows that in all cases the main product is sulfoxide except entry 12 in which sulfone is also produced as minor product. However, with increase in time, the formation of sulfone has not been observed for the other substrates. The primary hydroxyl group remained intact in the reaction (entry 8). Alkyl sulfides were also equally effective as substrates for the reaction (entries 6 and 11). Similarly, allylic sulfide gave the corresponding sulfoxide selectively in high yields without over-oxidation to sulfone, epoxidation or cleavage of double bond (entry 4). Nitrile and carbonyl groups were not also affected under these reaction conditions (entries 7, 9–12) (Table 3). We propose the mechanism of nano-sized Co<sub>2</sub>CrO<sub>4</sub> spinel catalyzed selective oxidation of sulfides to their corresponding sulfoxides in the presence of H<sub>2</sub>O<sub>2</sub> in Scheme 2.

One of the special features of nano-sized Co<sub>2</sub>CrO<sub>4</sub> spinel catalyst is its insolubility in organic solvents which makes its recovery very convenient. Therefore, the reusability of the catalyst was examined under the optimized reaction conditions with methyl phenylsulfide as a model reaction. For each of the repeated reactions, the catalyst was recovered, washed with ethylacetate consecutively and dried before being used for the next oxidation reaction. It is important to note that the catalyst was reused four times without any significant loss of activity and selectivity as shown in Fig. 7 and the structure of the nano-sized Co<sub>2</sub>CrO<sub>4</sub> spinel has not been changed.

A literature assay for the comparison of this method with some other previously reported ones including H<sub>2</sub>O<sub>2</sub> oxidation of methyl phenylsulfide demonstrates the efficiency of nano-sized Co<sub>2</sub>CrO<sub>4</sub> spinel catalyst for the selective oxidation as shown in Table 4.

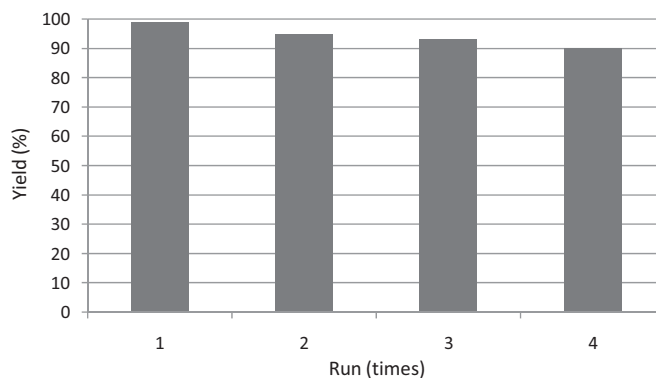
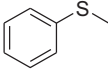
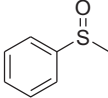
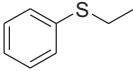
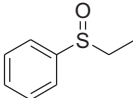
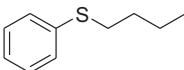
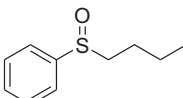
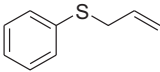
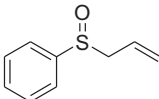
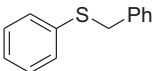
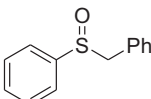
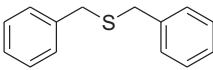
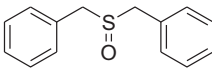
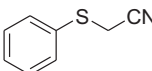
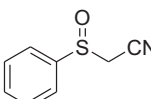
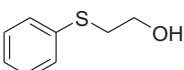
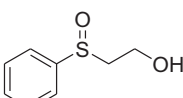
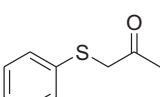
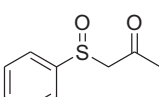
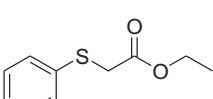
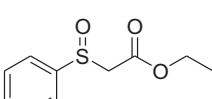
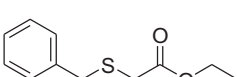
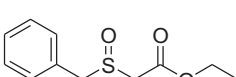
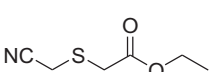
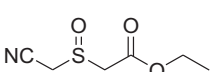


Fig. 7. Recycling of Co<sub>2</sub>CrO<sub>4</sub> spinel nanopowder in the selective oxidation reaction of methyl phenylsulfide to methyl phenylsulfoxide.

**Table 3**  
Oxidation of sulfides with H<sub>2</sub>O<sub>2</sub> in the presence of Co<sub>2</sub>CrO<sub>4</sub> spinel nanoparticles.<sup>a</sup>

Entry	Substrate	Time (min)	Product	Yield (%) <sup>b</sup>	TOF (h <sup>-1</sup> ) <sup>c</sup>
1		30		99	335
2		100		95	96.45
3		90		95	101.5
4		100		94	95.43
5		160		80	50.76
6		40		98	248.73
7		60		94	159.05
8		60		90	152.28
9		90		91	101.52
10		70		96	139.23
11		90		96	108.29
12		120		70	59.22

<sup>a</sup> All the reactions were carried out with 1 mmol of substrate, 1.1 mg of Co<sub>2</sub>CrO<sub>4</sub> spinel nanoparticles in 10 ml *t*-BuOH and 10 equiv. of 30% aqueous H<sub>2</sub>O<sub>2</sub> at room temperature.

<sup>b</sup> Yields were determined by <sup>1</sup>H NMR spectroscopy.

<sup>c</sup> Turnover frequencies (TOFs) defined as mmol of products reacted per mmol of catalyst per hour.

**Table 4**The comparison of some other catalyst with Co<sub>2</sub>CrO<sub>4</sub> spinel nanoparticles.

Entry	Catalyst	Weight (mg) <sup>a</sup> (mol%)	Temp. (°C)	Time (h)	Yield (%)		Literature
					Sulfoxide	Sulfone	
1	Na <sub>2</sub> WO <sub>4</sub> , C <sub>6</sub> H <sub>5</sub> PO <sub>3</sub> H <sub>2</sub> , [CH <sub>3</sub> (n-C <sub>8</sub> H <sub>17</sub> ) <sub>3</sub> N]HSO <sub>4</sub>	4.7 (0.1)	35	9	93	7	[23]
2	Tungstate-exchanged Mg–Al-LDH	200 (4.4) <sup>b</sup>	rt	0.5	88	12	[24]
3	Sc(OTf) <sub>3</sub>	9.8 (20)	rt	5	95	3	[25]
4	MoO <sub>2</sub> Cl <sub>2</sub>	12 (1.5)	rt	0.35	89	11	[26]
5	Silica sulfuric acid	100 (–)	rt	0.5	95	3	[27]
6	Carbon-based solid acid	200 (–)	Reflux	0.17	98	2	[28]
7	TaCl <sub>5</sub>	7.1 (2)	rt	2	90	10	[29]
8	Preyssler-type heteropolyacid modified nano-sized TiO <sub>2</sub>	25 (–)	rt	1	98	2	[30]
9	Co <sub>2</sub> CrO <sub>4</sub> spinel nanoparticles	1.1 (0.5)	rt	0.5	96	0	– <sup>c</sup>

<sup>a</sup> mg of the catalyst per 1 mmol of the methyl phenylsulfide.<sup>b</sup> mol% of WO<sub>4</sub><sup>2–</sup> content.<sup>c</sup> Reaction conditions as exemplified in the experimental procedure.

#### 4. Conclusions

In summary, nanoparticles of Co<sub>2</sub>CrO<sub>4</sub> spinel were prepared using sol–gel method in the presence of oxalic acid as a chelating agent. The XRD, EDX and TEM reveal that the Co<sub>2</sub>CrO<sub>4</sub> nanoparticles prepared by calcinating the gel precursor at 450 °C have good crystallinity in spinel structure. According to TEM image, the particle size of nano-sized Co<sub>2</sub>CrO<sub>4</sub> spinel was obtained at 9 nm. The nanoparticles exhibited regular morphology with homogeneous particle size distribution. The IR spectroscopy also confirms the desired structure of the nanoparticles.

Eventually, a simple, rapid, efficient and recyclable protocol for the selective oxidation of sulfides to their corresponding sulfoxides using Co<sub>2</sub>CrO<sub>4</sub> spinel nanoparticles with 30% H<sub>2</sub>O<sub>2</sub> in *t*-BuOH was evaluated. High yields, chemoselectivity and mild reaction conditions are the advantages of this method.

#### Acknowledgements

The authors gratefully acknowledge Ferdowsi University of Mashhad for financial support of this project (P438) and R. Pesian and N. Hashemian for taking TEM images at Central Laboratory of Ferdowsi University of Mashhad.

#### References

- [1] J. Ghose, R.C. Murthy, J. Catal. 162 (1996) 359–360.
- [2] N. Guilhaume, M. Primet, J. Chem. Soc., Faraday Trans. 90 (1994) 1541–1545.
- [3] X. Wei, D. Chen, W. Tang, Mater. Chem. Phys. 103 (2007) 54–58.
- [4] M. Bayhan, T. Hashemi, A.W. Brinkman, J. Mater. Sci. 32 (1997) 6619–6623.
- [5] Z.V. Marinkovic, L. Mancic, P. Vulic, O. Milosevi, J. Eur. Ceram. Soc. 25 (2005) 2081–2093.
- [6] A. Manthiram, J. Kim, Chem. Mater. 10 (1998) 2895–2909.
- [7] K.J. Omata, T.K.S. Takada, S.J. Kasahara, M.N. Yamada, Appl. Catal. A: Gen. 146 (1996) 255–267.
- [8] K.L. Zhang, J.B. Yuan, G.F. Zhu, Q.C. Zhang, J.T. Tang, J. Wuhan Univ. Nat. Sci. Ed. 4 (1997) 428–432.
- [9] A.G. Shi, A.H. Hang, J. Fang, J.S. Chi, M.M. Wu, Chin. J. Inorg. Chem. 5 (2001) 14–19.
- [10] M. Yazdanbakhsh, I. Khosravi, E.K. Goharshadi, A. Youssefi, J. Hazard. Mater. 184 (2010) 684–689.
- [11] K.W. Hanck, H.A. Laitinen, J. Inorg. Nucl. Chem. 33 (1971) 63–73.
- [12] E.L.S. Gomes, O.L. Casagrande, Thermochim. Acta 331 (1999) 87–91.
- [13] H.S. O'Neill, Rocks Miner. Mag. 67 (2003) 547–554.
- [14] H. Itoh, S. Utamapanya, J.V. Stark, K.J. Klabunde, J.R. Schlup, Chem. Mater. 5 (1993) 71–77.
- [15] J. Guzman, B.C. Gates, Nano Lett. 1 (2001) 689–692.
- [16] B.M. Choudary, M.L. Kantam, K.V.S. Ranganath, K. Mahender, B. Sreedhar, J. Am. Chem. Soc. 126 (2004) 3396–3397.
- [17] A. Fox, M.T. Dulay, Chem. Rev. 93 (1993) 341–357.
- [18] S. Anandan, A. Vinu, N. Venkatachalam, B. Arabindoo, V. Murugesan, J. Mol. Catal. A: Chem. 256 (2006) 312–320.
- [19] M.R. Hoffman, S.T. Martin, W. Choi, D.W. Bahnemann, Chem. Rev. 95 (1995) 69–96.
- [20] M. Rahimizadeh, Z. Bakhtiarpoor, H. Eshghi, M. Pordel, G. Rajabzadeh, Monatsh. Chem. 140 (2009) 1465–1469.
- [21] M. Rahimizadeh, M. Bakavoli, A. Shiri, H. Eshghi, Bull. Korean Chem. Soc. 30 (2009) 1699–1700.
- [22] M. Bakavoli, M. Rahimizadeh, H. Eshghi, A. Shiri, Z. Ebrahimpour, R. Takjoo, Bull. Korean Chem. Soc. 31 (2010) 949–952.
- [23] K. Sato, M. Hyodo, M. Aoki, X. Zheng, R. Noyori, Tetrahedron 57 (2001) 2469–2476.
- [24] B.M. Choudary, B. Bharathi, C.V. Reddy, M.L. Kantam, J. Chem. Soc. Perkin Trans. 1 (2002) 2069–2074.
- [25] M. Matteucci, G. Bhalay, M. Bradley, Org. Lett. 5 (2003) 235–237.
- [26] K. Jeyakumar, D.K. Chand, Tetrahedron Lett. 47 (2006) 4573–4576.
- [27] A. Shaabani, A.H. Rezayan, Catal. Commun. 8 (2007) 1112–1116.
- [28] A. Zali, A. Shokrolahi, M.H. Keshavarz, M.A. Zarei, Acta Chim. Slov. 55 (2008) 257–260.
- [29] M. Kirihara, J. Yamamoto, T. Noguchi, Y. Hirai, Tetrahedron Lett. 50 (2009) 1180–1183.
- [30] M. Rahimizadeh, G. Rajabzadeh, S.M. Khatami, H. Eshghi, A. Shiri, J. Mol. Catal. A: Chem. 323 (2010) 59–64.